PHYSICAL REVIEW B VOLUME 24, NUMBER 12 15 DECEMBER 1981

Radial distribution function and structural relaxation in amorphous solids

D. Srolovitz, T. Egami, and V. Vitek
Department of Materials Science and Engineering and Laboratory for Research on the Structure of Matter, University of Pennsylvania, Philadelphia, Pennsylvania 19104
(Received 13 April 1981; revised manuscript received 14 August 1981)

A method of interpreting radial distribution functions (RDF) of amorphous metals is proposed in which the role of the local atomic structure is emphasized. It is found that the width and height of the peaks of the RDF are related to the second moment of the atomic-level hydrostatic stress distribution $\langle p^2 \rangle$. The results of this analysis are then used to explain the details of the changes that occur in the RDF when structural relaxation takes place. The theoretical ΔRDF is found to be in excellent agreement with the results of a computer study and previous experimental results. It is further proposed that changes in $\langle p^2 \rangle$ may be most easily accounted for in terms of changes in the density of the structural defects defined in terms of the local fluctuations in the hydrostatic stress. In this way the changes that occur in the structure of amorphous metal during structural relaxation, as represented by the RDF, may be explained in terms of the motion and annihilation of these structural defects. It is concluded that the number density of defects which could account for the observed changes in the experimental RDF is 10%. It is also found that while the hydrostatic stress distribution may be significantly changed during structural relaxation, the distribution of the atomic-level shear stresses remains unaltered.

I. INTRODUCTION

Even after many years of careful study, the structure of amorphous alloys is far from being completely understood.[1] Experimentally, structural information may be extracted using x-ray, electron, and neutron scattering techniques, as well as Mössbauer or NMR measurements.[2] While the Mössbauer[3] or NMR[4] techniques provide indirect information on the local structure, direct structural information can be obtained only through the radial distribution function (RDF) determined by the scattering methods. However, RDF analyses still provide only averaged one-dimensional information about the locally varying three-dimensional structures[5,6] of the amorphous alloys. In order to better understand the structure in a nonaveraged manner, many workers were led to build hard-sphere models[7,8] as well as relaxed atomic models.[9–11] These models yield coordinates of a large number of atoms and have been analyzed in terms of the radial distribution function,[12] density,[13] polyhedral analysis,[5,14] and more recently in terms of the atomic-level stresses and site-symmetry coefficients.[6,15] While the density and RDF analyses provide only averaged information, the analyses using polyhedra, atomic-level stresses, and site-symmetry coefficients provide local information. Furthermore, it has been shown that the usefulness of the polyhedral analyses is rather limited relative to those of the atomic-level stresses.[16] Because of the wide applicability of the radial distribution function in studies of both experimental and model amorphous systems and owing to the power of the atomic-level stress analysis, we attempt to combine these two techniques to elucidate the changes that occur during structural relaxation.

Since amorphous alloys are generally obtained by rapid quenching, they are metastable, both with respect to crystallization and with respect to structural relaxation. Quenched samples are brought to more stable states by annealing at temperatures which do not lead to crystallization. As the alloy becomes relaxed, changes are experimentally observed (for a review, see Ref. 17). For example, these changes may be seen in the density,[18] Young's modulus,[18,19] Curie temperature,[20] electrical resistivity,[21] internal friction,[19] magnetic aftereffect,[22] embrittlement,[23] diffusion,[24] mechanical creep,[25] etc. In addition, small but distinct changes in the radial distribution function were observed, upon low-temperature annealing of metallic glasses.[26,27] Preliminary explanations of the changes in the RDF and the density during structural relaxation were discussed in Ref. 15.

In this paper we first review the definition of the

atomic-level stresses. The relationship between changes in the radial distribution function upon structural relaxation and the local hydrostatic stress fluctuations is then shown. Using these new concepts we analyze the results of an experimental annealing study and compare with those of a structural relaxation study in a model amorphous system. The results are analyzed in terms of the structural defects which lead to the first experimental determination of the defect concentration in amorphous metals. The implications of these results in relation to other physical properties are discussed.

II. LOCAL STRUCTURAL PARAMETERS

In a system of interacting particles, the application of a small uniform strain will result in a change of its energy. To first order, the change associated with the ith atom is

$$\Delta E_i = \Omega_i \sum_{\alpha\beta} \sigma_i^{\alpha\beta} \epsilon^{\alpha\beta} , \tag{1}$$

where $\epsilon^{\alpha\beta}$ is the $(\alpha\beta)$ component of the applied strain and Ω_i is the atomic volume of the ith atom. The coefficients $\sigma_i^{\alpha\beta}$ define the local atomic-level stress tensor at the position of atom i. If $\vec{f}_{ij}$ is the force between the ith and jth atoms this stress is

$$\sigma_i^{\alpha\beta} = \frac{1}{2\Omega_i} \sum_j f_{ij}^{\alpha} r_{ij}^{\beta} . \tag{2}$$

The vector $\vec{r}_{ij}$ is equal to $\vec{r}_i - \vec{r}_j$, where $\vec{r}_i$ and $\vec{r}_j$ are the position vectors of atoms i and j, respectively. When the forces between the atoms are described by a two-body potential $\phi(r)$, Eq. (2) can be written as[28]

$$\sigma_i^{\alpha\beta} = \frac{1}{2\Omega_i} \sum_j \frac{\partial\phi(r_{ij})}{\partial r_{ij}} \frac{r_{ij}^{\alpha} r_{ij}^{\beta}}{|r_{ij}|} . \tag{3}$$

In amorphous solids, the choice of the coordinate system is completely arbitrary while the stress tensor is explicitly dependent on this choice. Therefore, instead of the full tensor we concentrate on two rotational invariants of this tensor[15]

$$p \equiv \tfrac{1}{3}(\sigma_1 + \sigma_2 + \sigma_3) , \tag{4}$$

$$\tau \equiv \left[\frac{1}{3} \left[\frac{(\sigma_1-\sigma_2)^2}{2} + \frac{(\sigma_2-\sigma_3)^2}{2} + \frac{(\sigma_3-\sigma_1)^2}{2} \right] \right]^{1/2} , \tag{5}$$

where σ_1, σ_2, and σ_3 are the three principal stresses. The parameter p is obviously the local hydrostatic pressure, while τ is the average shear stress (von Mises's shear stress). The statistical distributions of p and τ are shown in Figs. 1 and 2, respectively, for a model amorphous structure of 2067 atoms, originally constructed by Maeda and Takeuchi,[11] using periodic boundary conditions and relaxed under the influence of a modified Johnson potential[29,15] for iron. The average value of p, $\langle p \rangle$, is almost zero since it corresponds to the macroscopic external pressure, but the root-mean-square value, $\langle p^2 \rangle^{1/2}$, is fairly large and is equal to about 10 GPa, which is about 6% of the bulk modulus B.

It is readily recognized that the value of $\langle p^2 \rangle$ may be related to the width of the first peak of the RDF. However, this relation is not straightforward, since the RDF represents only the two-body correlation while the distribution of p describes the fluctuation in the local density which, as explained below, is a more collective phenomenon. It follows from (3) and (4) that

$$\langle p^2 \rangle = I_1 + I_2 , \tag{6}$$

where

$$I_1 = \frac{1}{N} \sum_i \frac{1}{36\Omega_i^2} \sum_j \left[\frac{\partial\phi(r_{ij})}{\partial r_{ij}} \right]^2 r_{ij}^2 ,$$

$$I_2 = \frac{1}{N} \sum_i \frac{1}{36\Omega_i^2} \sum_{j \neq j'} \sum \frac{\partial\phi(r_{ij})}{\partial r_{ij}} \frac{\partial\phi(r_{ij'})}{\partial r_{ij'}} r_{ij} r_{ij'} .$$

N is the total number of atoms. Using the pair correlation function

$$\rho(r) = \frac{1}{N} \sum_{ij} \delta(r - r_{ij}) / r^2 , \tag{7}$$

I_1 can be approximately written as

$$I_1 \cong \frac{1}{36\langle \Omega^2 \rangle} \int \left[\frac{\partial\phi(r)}{\partial r} \right]^2 r^4 \rho(r) dr . \tag{8}$$

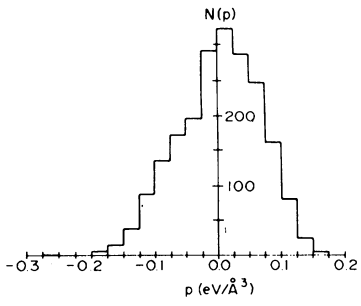

FIG. 1. Distribution histogram for the atomic-level hydrostatic stress p.

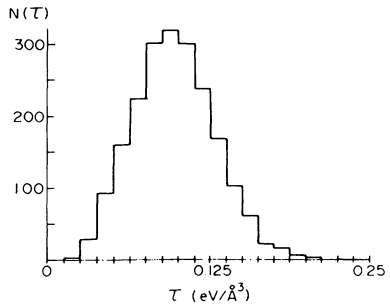

FIG. 2. Distribution histogram for the atomic-level shear stress τ.

While Eq. (8) shows that I_1 can be calculated with the knowledge of only the RDF and the interatomic potential, I_2 cannot be. The ratio I_2/I_1 is about 0.38 for our model. Therefore, the local density fluctuations described by the fluctuation in p contain significant collective components.[30]

III. RADIAL DISTRIBUTION FUNCTION ANALYSIS

We can examine the effect of the local density fluctuations on the radial distribution function by using the p distribution $N(p)$ of Fig. 1. First, we divide $N(p)$ into three sections; section 1 contains the 25% of the atoms subject to the largest compression, section 2 contains the 25% of the atoms subject to the largest tension, and section 3 contains the remaining atoms. The radial distribution function for each individual section is calculated as follows:

$$G(r)=4\pi r[\rho(r)-\rho_0]\ , \tag{9}$$

where ρ_0 is the average density and $\rho(r)$ is calculated by successively fixing the origin on each atom within the section and calculating the density of atoms at a distance r from this origin. In evaluating the density we consider all the atoms, not only those which belong to the specific section being considered. We then average these densitites to yield $\rho(r)$ and thereby $G(r)$ for the specific group. The radial distribution functions for the compressive and tensile sections are shown in Figs. 3(a) and 3(b). Figure 4 shows these two RDF's overlapped so as to match up the peaks for large values of r. Figures 3 and 4 show that the shape of the two RDF's are almost identical, but the RDF from the tensile section is shifted to larger values of r relative to that from the compressive section. The phase shift appears to be constant past the first

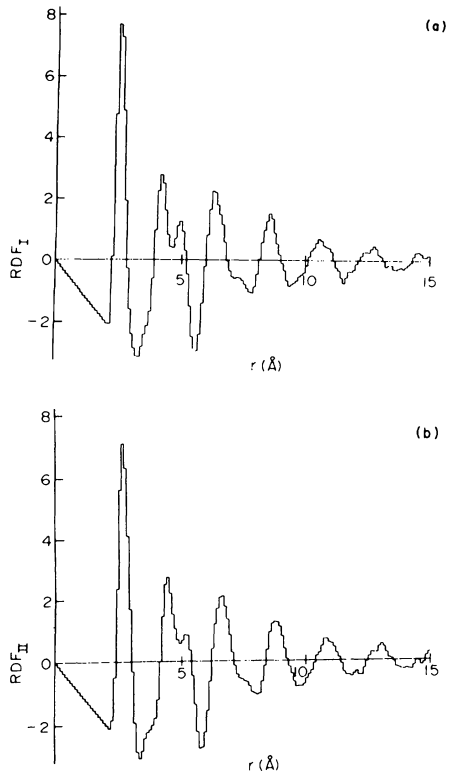

FIG. 3. Radial distribution functions for the 25% of the atoms subject to (a) the most compressive stresses and (b) the most tensile stresses.

peak, as shown schematically in Fig. 5. This indicates that the range of hydrostatic stresses is limited, on average, to first-nearest neighbors, since if there were a long-range hydrostatic stress field, the phase shift would be proportional to r^{-2}. This result can be expected in a one-dimensional system,

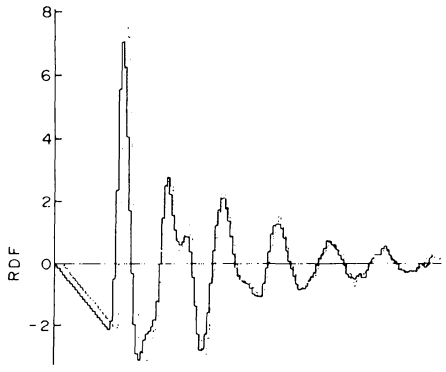

FIG. 4. Overlapping of two RDF's from Fig. 3 with the large r peaks matched. The dotted line is the RDF for the atoms in compression while the solid line is for those in tension.

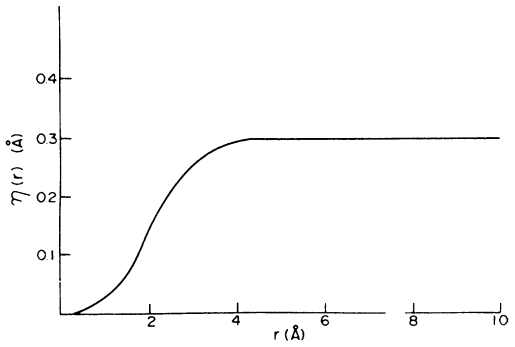

FIG. 5. Schematic illustration of the r dependence of the phase shift of the RDF.

but it is somewhat surprising in a three-dimensional system.

This simple relation among the RDF's for each section implies that $G(r)$ may be written as a function of p. To a good approximation the radial distribution function centered on the atoms with hydrostatic stress p can be expressed as

$$G_p(r)=G_0(r+\gamma p)\ , \tag{10}$$

where γ is constant beyond the first peak in $G(r)$, and $G_0(r)$ is the RDF from atoms with $p=0$. Expanding $G_0(r+\gamma p)$ into a Taylor's series about $p=0$,

$$G_0(r+\gamma p)=G_0(r)+\frac{\partial G_0(r)}{\partial r}\gamma p + \frac{1}{2!}\frac{\partial^2 G_0(r)}{\partial r^2}\gamma^2 p^2+\cdots\ . \tag{11}$$

The total radial distribution function $\langle G_0(r+\gamma p)\rangle$ is given by averaging $G_0(r+\gamma p)$ over the whole distribution of p values $N(p)$ that exist in the amorphous solid. To second order,

$$\langle G_0(r+\gamma p)\rangle = \int G_0(r+\gamma p)N(p)dp \Big/ \int N(p)dp \cong G_0(r)+\frac{\gamma^2}{2}\frac{\partial^2 G_0(r)}{\partial r^2}\langle p^2\rangle\ , \tag{12}$$

since $\langle p\rangle=0$ in this model.

We have calculated $G_0(r)$ by using the 10% of the atoms with the smallest hydrostatic stress, and $\partial^2 G_0(r)/\partial r^2$ by fitting two hundred cubic splines to $G_0(r)$ and evaluating the second derivatives explicitly.

IV. STRUCTURAL RELAXATION AND THE CHANGES IN THE RDF

The changes that occur in the radial distribution function when an as-quenched ribbon of amorphous metal is subjected to a low-temperature anneal have been examined using the energy-dispersive x-ray-diffraction method[26] and by conventional x-ray-diffraction techniques.[27] The result of the former study is shown in Fig. 6 for an amorphous $Fe_{40}Ni_{40}P_{14}B_6$ alloy. The change in the RDF is given as

$$\Delta\text{RDF}=\text{RDF(annealed)}-\text{RDF(as-quenched)} =4\pi r[\rho(r)_{\text{annealed}}-\rho(r)_{\text{as-quenched}}]\ . \tag{13}$$

It is observed that the effect of structural relaxation is to sharpen the peaks of the RDF without appreciably shifting them. It follows from Eq. (12) that it is then reasonable to assume that the distribution of p will also be sharpened, and the value of $\langle p^2\rangle$ reduced. We shall, therefore, attempt to interpret the changes in the RDF at first solely on the basis of the relaxation of the density fluctuations ($\langle p^2\rangle$). This approximation ignores all chemical effects and relegates all structural changes to pure radial or dilatational changes. This is not an unreasonable assumption since the angular changes that occur will average out to zero and the effect of changes in the chemical short-range order will not be seen because the metalloids are practically invisible in the x-ray studies and iron and nickel are very similar. Furthermore, we ignore the effect of shear stress fluctuations. This point will be discussed later.

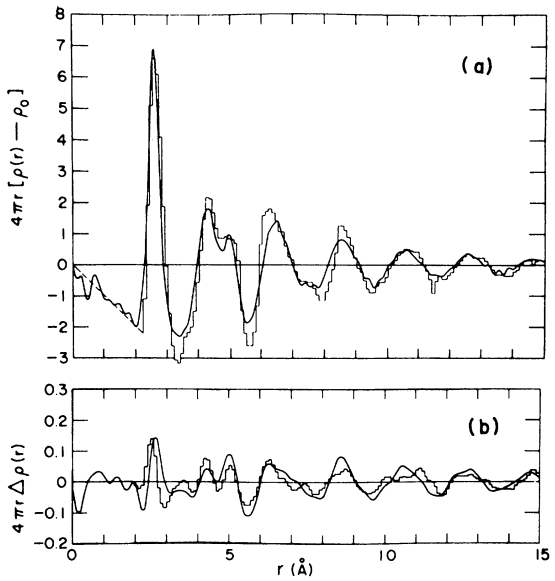

FIG. 6. (a) RDF for the whole model (histogram) overlayed on the experimentally measured $Fe_{40}Ni_{40}P_{14}B_6$ RDF (Ref. 26). (b) The ΔRDF, calculated using p and the symmetry coefficient α_0 (Ref. 15) (histogram), overlapped on the experimentally measured ΔRDF.

We then write

$$\Delta\text{RDF} = \langle G_0(r+\gamma p)\rangle_{\text{annealed}} - \langle G_0(r+\gamma p)\rangle_{\text{as-quenched}} . \quad (14)$$

Substituting from Eq. (12),

$$\Delta\text{RDF} \cong -\frac{\gamma^2}{2}\frac{\partial^2 G_0(r)}{\partial r^2}(\langle p^2\rangle_{\text{annealed}} - \langle p^2\rangle_{\text{as-quenched}}) . \quad (15)$$

This implies that the ΔRDF should be proportional to $-\partial^2 G_0(r)/\partial r^2$. Figure 6 shows the experimental ΔRDF, while Fig. 7(a) shows $-\partial^2 G_0(r)/\partial r^2$. The agreement is good past the first peak. The disagreement at the first peak is mainly due to the fact that the phase shift between the compressive and tensile regions is only constant past the first peak, as seen in Fig. 4, and is smaller for the first peak. The agreement between these two plots appears to justify the previous approximation.

In order to determine the value of γ for our model, we have simulated the change in $\langle p^2\rangle$ by simply excluding both edges of the distribution of p, as shown in Fig. 8. This has been done as follows: RDF(annealed) has been calculated as in (9) by centering the origin successively on those atoms which belong to the central part of the distribution of p, but considering all the atoms when evaluating the radial density. When calculating RDF(as-quenched) the origin has been centered successively on all atoms. The ΔRDF is then evaluated by using Eq. (13). The value of γ beyond the first peak of the RDF can then be calculated by using Eq. (15). The value of γ is dependent on the chosen cutoff used to exclude the edges of the p distribution, but is nearly constant when the concentration of the excluded atoms is low, as shown in Fig. 9.

Using these results, the experimental RDF was

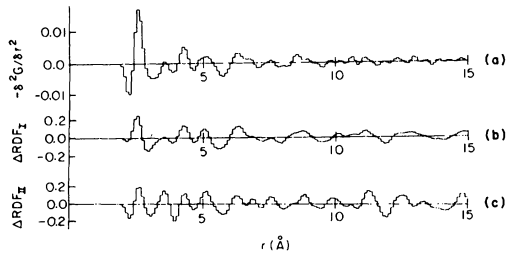

FIG. 7. Second derivative of the RDF of atoms subject to zero hydrostatic stress (a) with ΔRDF calculated using p and the symmetry coefficient α_0 (b) and that calculated using only p (c).

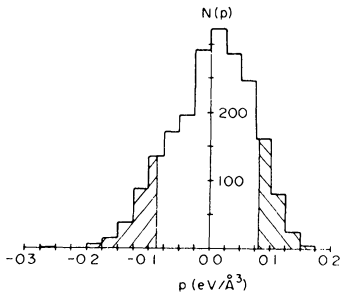

FIG. 8. Hydrostatic stress distribution, where the hatched areas on the left and right sides represented those atoms to be excluded.

analyzed. We may assume that the values of γ and $\partial^2 G_0(r)/\partial r^2$ evaluated for amorphous iron are still appropriate for the experimentally studied alloy in spite of the differences in composition, because of the similarities in the RDF and the elastic constants. If we set $\gamma = 2.3$ (Å^4/eV^2) as follows from the extrapolation of Fig. 9 to zero cutoff, the change in $\langle p^2\rangle$ corresponding to the experimental RDF is calculated to be

$$\Delta\langle p^2\rangle = \langle p^2\rangle_{\text{annealed}} - \langle p^2\rangle_{\text{as-quenched}} = -1.35\times 10^{-3}\ (\text{eV/Å}^3)^2 . \quad (16)$$

This corresponds to 32% of the value of $\langle p^2\rangle$ in the as-quenched state. This amount of reduction in $\langle p^2\rangle$ can be achieved by excluding 5% atoms from each end of $N(p)$ and renormalizing it to unity. The value of $\Delta\langle p^2\rangle$ may be slightly overestimated here, since in calculating the ΔRDF we neglected the change in G_0 due to annealing. It is noteworthy that the calculated value of $\Delta\langle p^2\rangle$ is much larger than the change in the square of the

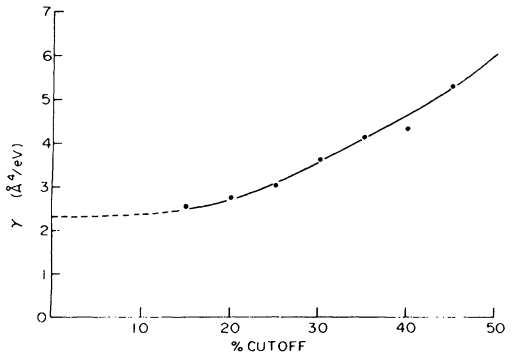

FIG. 9. Plot of the proportionality constant γ as a function of the percentage of atoms included in each type of LDF.

width of the first peak of the RDF, which is about 5%. Therefore, much of the change in $\langle p^2 \rangle$ comes from I_2, the correlated part.

In a previous paper,[30] we calculated the relationship between the local pressure p and the local atomic volume for the present model. The relation is

$$\Omega(p) = 9.476 + 9.788p + 15.712p^2 , \quad (17)$$

where Ω is in Å^3 and p is in eV/Å^3. The decrease in volume produced by such a change in $N(p)$ is about 0.3%. The decrease in volume observed during an annealing experiment similar to that used in producing the ΔRDF of Fig. 6, is indeed a little less than 0.3%,[20] which is in excellent agreement with our calculation.

We have examined so far the effect of the structural relaxation on the RDF considering only the changes in the distribution of the hydrostatic stress, $N(p)$. The atomic-level stresses, however, also have shear components, and the study would be incomplete without assessing the possiblity of a shear stress relaxation. For this purpose, we calculated ΔRDF assuming that the shear stresses on the 30% of the atoms with the largest shear stresses are relaxed, in a manner similar to that used in calculation of the ΔRDF for the relaxation in $\langle p^2 \rangle$. The results shown in Fig. 10 indicate that the ΔRDF due to the shear stress relaxation is considerably different from that for the pressure relaxation. The first peak in the ΔRDF is much larger than the higher-order peaks. Furthermore, the position of the peaks in the ΔRDF do not match correctly with those of the RDF, but are shifted slightly toward the larger values of r. This indicates that the ΔRDF has a component proportional to the first derivative of $G_0(r)$. This is a consequence of the weak linear correlation between τ and p.[15] The average pressure $\langle p \rangle$ is slightly negative when the value of τ is large, as shown in Table I. Therefore, when the shear stresses are relaxed, the volume may stay constant, or may even increase slightly[31] (see Table I). This result is contrary to the experimentally observed density changes. Together with the fact that the ΔRDF due to the shear stress relaxation (Fig. 10) does not agree with the experimental ΔRDF, it it suggested that the majority of the shear stress fluctuations do not become relaxed during the structural relaxation.

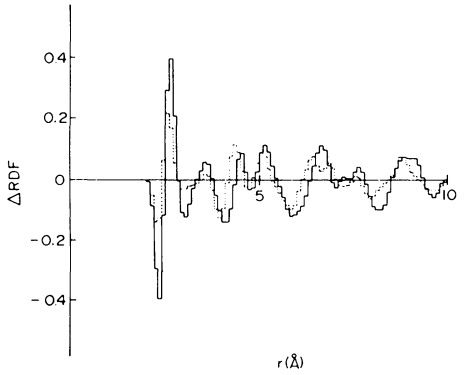

FIG. 10. Plot of the ΔRDF calculated using τ (solid line) and that using p and α_0 (dotted line).

V. STRUCTURAL DEFECTS IN AMORPHOUS SOLIDS

The experimental result shown in Fig. 6 indicates that the distribution of the interatomic distances becomes narrower upon annealing. In the last section we developed a relation between this narrowing of the interatomic distance distribution and the narrowing of the distribution of the atomic-level pressures. This relation is not trivial, as it might seem to be, since the atomic-level pressure represents not only the pair-wise atomic correlations but also some higher-order correlations as we discussed earlier.

For instance, an attempt has been made to simulate the experimental ΔRDF by a statistical narrowing of the distribution of interatomic distances.[33] The simulated ΔRDF closely resembles

TABLE I. The correlation coefficients between the local volume V and the shear stress τ and between p and τ, for atoms subject to small, medium, and large values of τ. The correlation coefficient is 1 for perfect correlation, 0 for no correlation, and −1 for perfect anticorrelation. The average values of V and p for each τ division are also shown.

	Correlation coefficient	Average value of parameter
τ(0−33%) V	0.0033	9.479 Å^3
p	−0.0536	0.0132 eV/Å^3
τ(34−66%) V	−0.0143	9.479 Å^3
p	−0.0379	0.0043 eV/Å^3
τ(67−100%) V	−0.0283	9.475 Å^3
p	−0.1715	−0.0097 eV/Å^3

$\partial^2 G_0(r)/\partial r^2$, as expected, so that the narrowing of the first peak of the RDF is grossly overestimated. This is because the correlations among the changes in the interatomic distances are not considered in this simulation. The atomic-level pressure, on the other hand, shows greater promise in describing the changes in the RDF realistically, since the correlations can be included through the r dependence of the phase-shift factor γ. Figure 7(c) was calculated by excluding 15% of atoms from both ends of the pressure spectrum, which we may tentatively call the defects, just as has been done in calculating the value of γ. The height of the first peak of the RDF is certainly much lower than that of $\partial^2 G_0(r)/\partial r^2$, and its relative height with respect to the other peaks is close to that of the experimental ΔRDF. The agreement with the experiment becomes even better if we further include α_0, one of the site-symmetry coefficients which is related to the local elastic constants,[16] in defining the defects. If the atoms constituting the defects are identified with those atoms which belong to the edges of both the pressure and α_0 distribution spectra, the calculated ΔRDF [Fig. 7(b)] shows an excellent agreement with the experimental ΔRDF as shown in Fig. 6. The pressure and α_0 are strongly correlated,[15] but apparently the combination of the two is most effective in identifying those atoms which take part in the relaxation during annealing. Furthermore, the total exclusion of both edges of the distribution leaves sharp and unnatural cuts in the distribution. On the other hand, by combining p and α_0 in defining the defects, the p distribution after removing the defects still remains smooth, as shown in Fig. 11.

In calculating the ΔRDF, we did not actually relax the structure, since an extremely large amount of computer time is required to carry out a realistic simulation of the relaxation, for instance, by a molecular dynamics technique. Instead, we assumed that the atomic rearrangements during the relaxation are strongly localized so that the total RDF can be considered to be merely a superposition of the local RDF's which are characterized by p, and are mutually independent. This assumption is crucial to our description of the amorphous structure. Its validity is supported by the agreement in the calculated and measured ΔRDF's. The most important basis of this assumption is the absence of a spatial correlation among the local pressures when averaged over the whole block (see Table II). However, this does not imply that isolated regions of correlated pressures do not exist.[15] This implies that the atomic-level pressure of one atom can be changed with only a small effect on other atoms. This localized nature of the pressure fluctuation suggests that the earlier tentative use of the term "defect" is justified. Since the fluctuations in p correspond to the fluctuations in specific density, we may call the region defined by a large tensile pressure and a small value of α_0 as a negative local-density fluctuation (n-type LDF), and the region with a large compressive pressure and a large value of α_0 as the positive LDF. Similarly we can define the τ defect as the shear stress concentration.[15] The threshold values used to define the defects cannot be determined *a priori*, but they may be estimated by comparing the quantities calculated on the basis of the model with the experimental ones. In the case of the p- and n-type LDF's, the comparison of the RDF's provide such a determination. As has been shown earlier, the experimentally observed change in the RDF corresponds to the exclusion of 5% of atoms from either edge of the p distribution. This means that the density of the p- and n-type LDF's which are annihilated during the relaxation is 5% each. While the details of the mechanisms of motion and annihilation of the defects are not known at

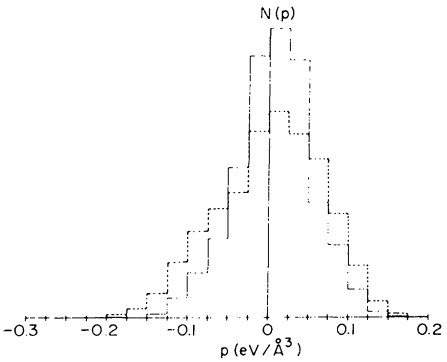

FIG. 11. Distribution histogram for the atomic-level hydrostatic stress p for the entire model (dotted line) and assuming atoms corresponding to both extreme values of p and α_0 are removed (solid line).

TABLE II. The correlation in p between each atom and all of their first-, second-, or third-nearest neighbors, as defined by the corresponding peaks in the RDF.

Neighbor	$\langle p_i p_j \rangle$ (eV/Å^3)^2	$\langle p_i p_j \rangle / \langle p^2 \rangle$
1st	7.27×10^{-4}	1.75×10^{-2}
2nd	1.05×10^{-4}	0.25×10^{-2}
3rd	0.83×10^{-4}	-0.20×10^{-2}

present, it is unlikely the LDF's simply dissipate because this would lead to larger density changes than those observed experimentally. Rather the p- and n-type LDF's mutually annihilate, producing no first-order changes in the density.

It was suggested in this study that the τ defects are not likely to be annealed out during the structural relaxation. This appears to be related to the different thermodynamical behaviors of the p and τ fluctuations, and will be discussed in more details elsewhere. This insensitivity of shear stress fluctuations to annealing provides additional support to our method of analyzing the RDF. The widths of the peaks of the RDF are determined not only by the p fluctuations but also by the τ fluctuations. Hence even when we succeed in arranging the atoms such that the pressure is zero everywhere, the peak widths of the RDF remain finite. This provids a justification of our assumption that $G_0(r)$ is independent of the change in the p distribution during the relaxation.

VI. CONCLUSIONS

The new method of analyzing radial distribution functions presented in this paper represents an attempt to examine the details of the RDF in terms of local atomic structure. It was shown that the role of the hydrostatic stress p can be described in terms of phase shifts in the RDF; compression produces shift towards smaller r values and tension towards larger r values. When the radial distribution function $G_p(r)$ is averaged over all atoms in the sample the effect of the distribution of p values is to decrease the sharpness of the peaks and smooth out some of the detail. The wider the p distribution, or equivalently the larger $\langle p^2 \rangle$, the more severe is the smoothing. Furthmore, the width of the p distribution provides an indication regarding the degree of the structural relaxation of the amorphous solid: Narrow p distributions correspond to well relaxed states, while wider distributions indicate unrelaxed states.

The change in the p distribution during the relaxation may be described in terms of the structural defects defined by the atomic-level stresses. The recombination of p-type (compressive) and n-type (tensile) defects account for the changes in density and for most of the changes in the RDF observed upon annealing. The τ defects (shear defects) were found to be largely unaffected by the structural relaxation. The agreement between the theoretical, experimental, and computer model results for structural relaxation allowed us to determine for the first time the defect density in a real amorphous solid. It was found that the annealing of amorphous $Fe_{40}Ni_{40}P_{14}B_6$ for 30 min at 350 °C led to the recombination of a total defect density of approximately 10%.

ACKNOWLEDGMENT

This research was supported by the National Science Foundation through the Material Research Laboratory Section Contract No. DMR79-23647.

[1]G. S. Cargill III, in *Solid State Physics*, edited by H. Ehrenreich, F. Seitz, and D. Turnbull (Academic, New York, 1975), Vol. 30, p. 227.
[2]C. N. J. Wagner, J. Non-Cryst. Solids 31, 1 (1978).
[3]I. Vincze, D. S. Boudreaux, and M. Tegze, Phys. Rev. B 19, 4896 (1979).
[4]P. Panissod, D. Aliaga Guerro, A. Amamov, J. Durard, W. L. Johnson, W. L. Carter, and S. J. Poon, Phys. Rev. Lett. 44, 1465 (1980).
[5]J. L. Finney, Proc. R. Soc. London Ser. A 319, 479 (1970).
[6]T. Egami, K. Maeda, and V. Vitek, Philos. Mag. A41, 883 (1980).
[7]J. D. Bernal, Proc. R. Soc. London Ser. A 280, 299 (1964).
[8]C. H. Bennett, J. Appl. Phys. 43, 2727 (1972).
[9]L. V. Heimendahl, J. Phys. F 5, L141 (1975).
[10]A. Rahman, M. J. Mandell, and J. P. McTague, J. Chem. Phys. 64, 1564 (1976).
[11]K. Maeda and S. Takeuchi, J. Phys. F 8, L283 (1976).
[12]D. S. Boudreaux, Phys. Rev. B 18, 4039 (1978).
[13]T. Anyo, H. Ohno, K. Kawamura, and F. Furukawa, Phys. Status Solidi, A 51, 325 (1979).
[14]Y. Yamamoto and M. Doyama, J. Phys. F 9, 617 (1979).
[15]D. Srolovitz, K. Maeda, V. Vitek, and T. Egami, Philos. Mag. A44, 847 (1981).
[16]D. Srolovitz, K. Maeda, S. Takeuchi, T. Egami, and V. Vitek, J. Phys. F 11, 2209 (1981).
[17]T. Egami, Ann. N. Y. Acad. Sci. 371, 238 (1981).
[18]H. S. Chen, J. Appl. Phys. 49, 3289 (1978).
[19]H. S. Chen, H. J. Leamy, and M. Barmatz, J. Non-

Cryst. Solids 5, 444 (1971).
[20]H. H. Liebermann, C. D. Graham, Jr., and P. J. Flanders, IEEE Trans. Magn. 13, 1541 (1977).
[21]M. Marcus, Acta Metall. 27, 879 (1979).
[22]P. Allia and F. Vinai, J. Phys. (Paris) 41, C8-645 (1980).
[23]R. S. Williams and T. Egami, in *Rapidly Quenched Metals III,* edited by B. Cantor (The Metals Society, London, 1978), Vol. 1, p. 214.
[24]H. S. Chen, L. C. Kimerling, J. M. Poate, and W. L. Brown, Appl. Phys. Lett. 32, 468 (1978).
[25]R. Maddin and T. Masumoto, Mater. Sci. Eng. 9, 153 (1972).
[26]T. Egami, J. Mater. Sci. 13, 2587 (1978).
[27]Y. Waseda and T. Egami, J. Mater. Sci. 14, 1249 (1979).
[28]M. Born and K. Huang, *Dynamical Theory of Crystal Lattices* (Clarendon, Oxford, 1954).
[29]R. A. Johnson, Phys, Rev. 134A, 1329 (1964).
[30]T. Egami, K. Maeda, D. Srolovitz, and V. Vitek, J. Phys. (Paris) 41, C8-272 (1980).
[31]The removal of 10% of the atoms with the largest values of τ will also result in an increase in p due to the p-τ correlations. The changes in p can be related to changes in the local atomic volume through Eq. (17). The decrease in the density thus produced is larger than the changes in the local atomic volume by a factor of 1.5 (Ref. 32), due to the interaction with the lattice, and is approximately 0.5%.
[32]J. D. Eshelby, Proc. R. Soc. London Ser. A 241, 376 (1957).
[33]H. Hermann, N. Mattern, and S. Kobe, Phys. Status Solidi B 99, 565 (1980).